Tribological performance of silicon nitride and carbon black Ionanofluids based on 1-ethyl-3-methylimidazolium methanesulfonate

Javier P. Vallejo[1,*], José M. Liñeira del Río[2], Josefa Fernández[2], Luis Lugo[1]

[1]Departamento de Física Aplicada, Facultade de Ciencias, Universidade de Vigo, E-36310 Vigo, Spain
[2]Laboratory of Thermophysical Properties, Nafomat Group, Department of Applied Physics, Faculty of Physics, University of Santiago de Compostela, 15782 Santiago de Compostela, Spain

*To whom correspondence should be addressed (Tel.: +34 986813771, E- mail: jvallejo@uvigo.es)

Abstract

Development of nano-lubricants by the dispersion of nano-particles in current lubricants has contributed to improving energy efficiency reducing wear and friction. During the last two decades, ionic liquids have evolved as novel lubricants or lubricant additives, especially for high vacuum and high temperature. Nevertheless, the number of experimental studies regarding the tribological properties of Ionanofluids, defined as dispersions of nano-particles in ionic liquids, is limited. 1-ethyl-3-methylimidazolium methanesulfonate, [EMIM][MS], is a promising candidate for lubrication applications due to its wide liquid range, high thermal conductivity, low friction coefficients and low compressibility in comparison with commercial mineral and synthetic hydrocarbon based lubricants. In this work, Ionanofluid lubricants based on dispersions of nano-additives (silicon nitride and carbon black) at mass concentration between 0.10 to 1.0 wt% in [EMIM][MS] were designed. The nearly spherical morphology of the nano-additives, silicon nitride and carbon black, was described by using scanning electron microscopy. The stabilities of the resulting nano-particle dispersions in ionic liquids were analyzed by dynamic light scattering measurements of size for one month. Tribological characterization was performed by a rotational rheometer coupled with a tribology cell with ball-on-three-pins configuration (100Cr6 steel) in sliding conditions at 298.15 and 353.15 K. Afterwards, the wear track morphology of the worn pins was analyzed by a 3D optical profiler and Raman Spectroscopy. The dispersions at the optimal nano-additive concentrations for lubrication reached friction coefficient decreases of up to 16% and wear tracks with a volume 28 times lower. Additionally, the density and dynamic viscosity of [EMIM][MS] and the optimal Ionanofluids for lubrication applications measured with a rotational Stabinger visco-densimeter in the 278.15 to 373.15 K temperature range show small increases with almost no dependence on temperature.

Keywords

tribological properties; 1-ethyl-3-methylimidazolium methanesulfonate; friction; Ionanofluids; nanolubricants.

1. Introduction

Nanofluids, dispersions of nano-sized solid particles in a conventional fluid, were initially conceived as a solution to enhance the thermal properties of classic heat transfer fluids [1, 2]. Nevertheless, the use of nano-particles as additives has also contributed to improving the tribological efficiency of common lubricants [3, 4]. Several studies have experimentally verified important reductions of the friction coefficient and wear volume by dispersing diverse nano-materials (metals, oxides, nitrides, carbon-based structures) in conventional lubricants in the past decade, as summarized various recent reviews [4-6]. Singh et al [6] summarized the physical phenomena described in the literature to improve the lubrication performance of the base fluid by the nano-particle addition: rolling mechanism, mending mechanism, polishing mechanism and protective film (Figure 1). Rolling effect assumes that nano-additives work like ball bearings, rolling between the two solid surfaces. Mending effect considers that the nano-additives fill the small grooves and repair microdamages of friction surfaces. Polishing mechanism considers that hard nano-additives act as polishers by eliminating asperities, hence, diminishing surface roughness. Finally, protective film effect assumes that nano-particles create a lubricating layer on the friction surface, preventing the direct contact between metallic elements [6, 7].

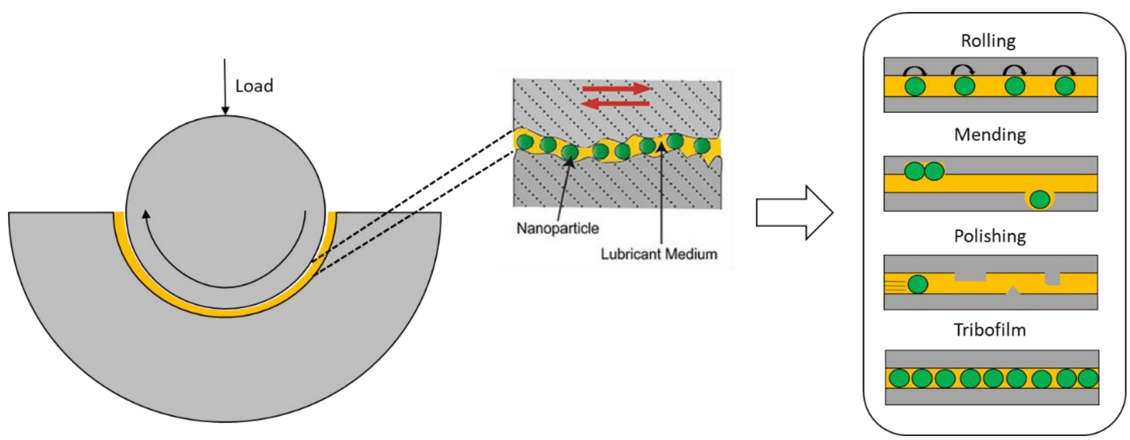

Figure 1. Schematic diagram representing the lubrication physical phenomenon and the lubrication mechanisms of nano-particles as additives.

Ionic liquids, IL, are organic salts in liquid state composed only of ions and with melting points lower than 100 ºC [8]. Those called room-temperature ILs melt below room-temperature. Their low melting points and negligible vapor pressure made them revolutionary in industry. They can be found in several applications such as heat transfer, absorption, sealant, lubricant or pressure transmission agents [9]. Specifically over the last two decades, ILs have been examined as novel lubricants [10] or lubricant additives [11, 12] due to their greater thermal stability, broader liquid range, lower volatility, lower flammability, higher thermal conductivity, and lower sensitivity to environmental variations in rheological behavior than conventional lubricants, among other interesting characteristics [12, 13]. ILs have been considered adequate as lubricants for extreme environments such as high vacuum and high temperature. Moreover, some ILs may constitute an environmental and health friendly alternative in comparison to traditional anti-wear additives (ZDDP) [13, 14].

The combination of the concepts of nanofluid and ionic liquid leads to the idea of Ionanofluids, which can be defined as dispersions of nano-particles in ionic liquids. This term was first proposed in 2009 [15] and since then, the scientific concern about these nano-dispersions has continuously increased [16, 17], mainly being used as heat transfer fluids [18, 19]. Nevertheless, many of the favorable lubrication mechanisms and properties described for both nanofluids (potential rolling, mending, polishing and protective film effects) and ionic liquids (protective film, interesting thermal and rheological properties, high vacuum and temperature adequacy, less harmful alternative for the environment and health) can show promising synergistic results.

There are few studies in the literature regarding the use of Ionanofluids for lubrication. Concerning studies examining Ionanofluids directly as lubricating agents, some literature examples and their main conclusions are summarized as follows. Initially, different authors [20-23] used ILs with hexafluorophosphate ([PF_6]) and tetrafluoroborate ([BF_4]) anions, but their reactivity with water produces corrosive hydrogen fluoride, so the applicability of these Ionanofluids as lubricants is restricted [24-26]. Khare et al. [27] synthesized and tribologically characterized at room temperature two different dispersions of graphene in 1-butyl-3-methylimidazolium iodide, [BMIM][I], obtaining slight reductions of the friction coefficient, wear, and roughness surface, in comparison to the neat IL. These behaviors were attributed to three main mechanisms: rolling, sliding, and exfoliation and film effects. The authors conclude that the rolling (due to nano-particles) and sliding (due to aggregates) phenomena compete between them when aggregates begin to appear and that the ball rolling effect is less effective for square-shaped nano-particles than for spherical nano-particles. Kheireddin et al. [28] studied the tribological properties at room temperature of SiO_2 nano-particles as additives of 1-butyl-3-methylimidazolium (trifluoromethysulfony)imide, [BMIM][TFSI], observing that the best anti-friction and anti-wear behavior were achieved for the optimum NP concentration (0.05 wt%), with a wear reduction of 24%. These improvements were ascribed to the enhanced loading capacity of the IL by the presence of SiO_2 nano-particles and to the capacity of the nano-particles to fill valleys between asperities (polishing mechanism). Yegin et al. [29] investigated the tribological behavior at room temperature of functionalized SiO_2 dispersions in 1-butyl-3-methylimidazolium bis(trifluoromethylsulfonyl)imide, [BMIM][NTf_2], reaching the higher friction coefficient reduction, 37%, for the 0.1 wt% concentration. This enhancement was attributed to the roller bearing effect of spherical SiO_2 nano-particles. Carrión et al. [30] and Espejo et al. [31] analyzed the tribological properties at room temperature of 0.5 wt% single-walled CNT and 0.5 wt% multi-walled CNT in 1-octyl-3-methylimidazolium chloride ([OMIM][Cl]) and 1-ethyl-3-methylimidazolium tosylate ([EMIM][TOS]), respectively. These authors obtained negligible wear surfaces and friction coefficients, with great reductions of 66 and 54% with respect to neat IL, respectively. These reductions were attributed to the improved load-carrying capacity of the dispersion and its enhanced ability to separate the sliding surfaces (explained by the interactions between nano-additives and IL molecules). From the same group, Saurín et al. [23, 32] obtained tribological characterizations at room temperature for 0.1 wt% few layer graphene and 0.1 wt% nano-diamonds dispersions in protic ammonium carboxylate tri-[bis(2-hydroxyethylammonium)] citrate [32]. Graphene dispersion led to slight reductions of the IL friction coefficient for full-fluid and thin layer lubrication, while nano-diamond dispersions lead to a 30% reduction. The graphene-IL dispersion covers the sliding path with a protecting layer that prevents wear, whereas this anti-wear effect is not observed for nano-diamonds. Besides, Pamies et al. [33] studied the tribological performance of 0.5 to 1 wt% graphene dispersions in [EMIM] dicyanamide ([DCA]) and [EMIM][TFSI] at room temperature. They obtained maximum reductions of 11 and 40% in friction and wear, respectively, for [EMIM][DCA], and a maximum friction reduction of 11% for [EMIM][TFSI]. The higher lubrication was attributed to three main reasons: the superior load-carrying ability of the dispersions, the formation of a surface layer of graphene deposited on the wear track, and the ability of graphene sheets to retain the nano-sized wear debris, preventing the creation of larger abrasive agglomerates.

As observed, the literature of Ionanofluids for lubrication applications usually describe tribological properties at room conditions. Therefore, comprehensive experimental analyses are needed to evaluate the effect of temperature variation. Moreover, most of the research on Ionanofluid lubricants has focused on the use of halogen-containing ionic liquids, which can cause negative effects on the environment [8, 34]. The delay in the development of industrial applications of the very promising research results obtained with Ionanofluid lubricants could be attributed to several factors, one of the most relevant is doubtless the problems of agglomeration of the nano-particles [34, 35], which can change the lubrication regime and increase wear due to abrasion. For this reason, as Avilés et al. [34] pointed out, there is an urgent need to optimize the nano-additive concentration, not only to achieve long-term stability, but also to control its influence on the thermophysical and tribochemical properties of the nanofluid. Hence, the aim of this work is to obtain the optimal concentration of two nano-additives for a non-halogenated ionic liquid, analyzing the tribological and thermophysical behavior at different temperatures.

The non-halogenated IL 1-ethyl-3-methylimidazolium methanesulfonate, [EMIM][MS], has been chosen due to the much lower isothermal compressibility and lower friction coefficients than those of commercial hydraulic fluids and compressor lubricants [36]. Furthermore, its thermal conductivity, 0.20 $W \cdot m^{-1} \cdot K^{-1}$ at 273 K [37], is higher than that usually reported for mineral and synthetic hydrocarbon based lubricants, 0.14 $W \cdot m^{-1} \cdot K^{-1}$ at 273 K [38], which implies a greater capacity to dissipate heat, one of the main functions of the lubricants. Recently, Bioucas et al. [37] concluded that the chemical structure and intermolecular interactions that characterize this IL lead to exceptional properties, which allow for heat transfer, among other applications. In addition, [EMIM][MS] has a wide liquid temperature range, with its freezing point at around 250 K [39]. The value of its kinematic viscosity at 313 K has been reported as 54.4 cSt [40].

To the best of the authors' knowledge, there are no previous experimental works in the literature analyzing the performance of [EMIM][MS] as a novel lubricant. In this work, the friction coefficient in sliding conditions between steel surfaces and the corresponding wear tracks of [EMIM][MS] were analyzed at two different controlled temperatures, 298.15 and 353.15 K, to study the temperature dependence. Furthermore, silicon nitride and carbon black, two nano-additives with different promising characteristics to improve the tribological performance of a lubricant and a relatively low production cost, have been employed to design [EMIM][MS]. Silicon nitride nano-particles are characterized by their resistance to oxidation at high temperatures, wear, and corrosion resistance. In addition, Çöl et al. [41] have found that silicon nitride nano-particles reduce the friction coefficient of an engine oil up to around 30% for 0.8 wt % concentration and the specific worn rate up to 40% for 0.1 wt% concentration. Ionanofluids in the 0.10 to 1.0 wt% concentration range. The appearance of the optimal concentration for each nano-additive and the different physical mechanisms involved in the improvement of tribological performance is one of the objectives of this work. Moreover, the morphology of the nano-additives and the stability of the resulting dispersions were analyzed. Then, the Ionanofluid lubricants were tribologically characterized, analyzing the friction coefficient at 298.15 and 353.15 K and characterizing the corresponding wear tracks. Elemental mapping and Raman spectra of the worn surfaces contributed to the physical interpretation. Additionally, the density and dynamic viscosity of the base IL and the optimized nano-additive dispersion for lubrication applications were also experimentally determined in a wide temperature range.

2. Materials and methods

2.1. Design

The ionic liquid 1-ethyl-3-methylimidazolium methanesulfonate, [EMIM][MS], was provided by Merck (Darmstadt, Germany) with a purity ≥ 95% and a water content < 0.5 wt%, see Table 1. Silicon nitride, Si_3N_4, and carbon black, CB, were provided by PlasmaChem (Berlin, Germany) with purities > 99%, see Table 1. The Ionanofluid lubricants, dispersions of Si_3N_4 and CB at three mass concentrations (0.10, 0.25 and 1.0 wt%) in [EMIM][MS], were prepared following a two-step method. The amounts of IL and each nano-additive used were weighted in a CPA225 balance from Sartorius AG (Goettingen, Germany) with 0.1 mg uncertainty. Subsequently, the dispersions were sonicated through an ultrasonic bath Fisherbrand FB11201 from Thermo Fisher Scientific (Waltham, MA, USA) for 120 min, operating in continuous shaking mode with an effective power of 180 W and a sonication frequency of 37 kHz.

Table 1. Main characteristics of materials used, according to the manufacturer[1,2].

Ionic liquid	**1-ethyl-3-methylimidazolium methanesulfonate[1], [EMIM][MS]**
CAS Number	145022-45-3
Other common nomenclature	[EMIM] [$MeSO_3$] [EMIM] [CH_3SO_3] [C2MIM][MS] [C_2mim][CH_3SO3]
Chemical structure	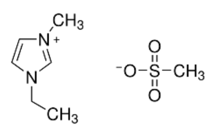 $C_7H_{14}N_2O_3S$
Flash point	559.15 K
Purity	≥ 95%
Water content	< 0.5 wt%
Nano-additive	**Silicon nitride[2], Si_3N_4**
Average particle size	25 nm
Specific surface area	75 $m^2 \cdot g^{-1}$
Purity	> 99%
Other contents	Fe < 0.05, Ca < 0.05, Al < 0.1%
Nano-additive	**Carbon black[2], CB**
Average particle size	13 nm
Specific surface area	550 m^2/g
Purity	> 99%
Other contents	Ash < 0.02%

[1]Merck (Darmstadt, Germany)
[2]PlasmaChem (Berlin, Germany)

2.2. Experimental

The nano-particles used were morphologically characterized through scanning electron microscopy (SEM). A drop of each dispersion composed of each nano-powder in analytical grade methanol was dried at room temperature on a silica support.

Backscattering electron images over the specimens were obtained by a JEOL JSM-6700F field emission scanning electron microscope from JEOL (Tokyo, Japan) at an operating accelerator voltage of 10.0 kV.

The stability of the ionic dispersions was analyzed by dynamic light scattering (DLS) technique through a Zetasizer Nano ZS from Malvern Instruments (Malvern, United Kingdom). The temporal evolution of the apparent size of the nano-additives was characterized with the procedure previously described [42, 43]. The present study was carried out for the 0.25 wt% Ionanofluids, the least concentrated dispersions, for 31 days at 298.15 K with a scattering angle of 173º. Two types of samples were analyzed: dispersions in static conditions since their preparation (from now on referred to as “static” samples) and dispersions to which mechanical agitation was applied before the DLS measurement (from now on referred to as “shaken” samples). The mechanical agitation of the shaken samples was performed with a ZX3 Advanced Vortex Mixer from VELP Scientifica (Usmate Velate, Italy) during 1 min at 2000 rpm.

The tribological characterization was conducted by a rotational rheometer MCR 302 from Anton Paar (Graz, Austria) coupled with a tribology cell T-PTD 200 at 298.15 and 353.15 K [44, 45]. The temperature was controlled with a Peltier system H-PTD 200 with 0.1 K accuracy. A ball-on-three-pins configuration was employed for the tests. The 100Cr6 steel ball is 12.7 mm in diameter and the 100Cr6 steel pins have a diameter of 6 mm and are 6 mm high. Before each test, all materials were cleaned by means of hexane and dried in atmospheric conditions. 1.3 mL of sample per test was used, ball and pins being completely submerged. The operating parameters were 45 N total axial force of the rheometer (21.20 N normal force at each pin-ball surface contact, 0.7 GPa average contact pressure), 0.1 $m \cdot s^{-1}$ constant sliding velocity and 340 m sliding distance. Three replicates were run for each dispersion. More information about the tribological cell and the procedure can be found elsewhere [44, 45].

The surface morphology of the worn pins generated after the tribological tests was analyzed by a 3D optical profiler S neox from Sensofar (Tarrasa, Spain) [46, 47]. 3D images of the wear of the pins as well as the wear scar diameter, the wear track depth and wear hole volume were obtained in confocal mode with a 10x objective. This apparatus was also used to evaluate the roughness (Ra) of the worn surfaces of the pins lubricated with the studied samples. For this task, the ISO4287 standard (International Organization for Standardization, Vernier, Switzerland) was followed, employing a Gaussian filter with a long wavelength cut-off of 0.08 mm and 0.25 mm. The presented values of wear scar diameter, the wear track depth, wear hole volume and roughness were obtained as the average of the three replicates for each nano-additive concentration. Elemental mapping and Raman spectra of the worn surfaces were recorded with a confocal Raman microscope alpha 300R+ from WITec (Ulm, Germany) at a wavelength of 532 nm in order to obtain information about the composition in the wear track.

Dynamic viscosities were determined by a rotational Stabinger viscometer SVM 3000 from Anton Paar (Graz, Austria) at atmospheric pressure and in the temperature range from 278.15 to 373.15 K, 5 K step. This device also includes a vibrating tube densimeter that determines the densities at the same conditions. More information of this setup was previously described [48, 49]. The expanded uncertainty of these measurements (0.95 level of confidence) was previously established as 1% for dynamic viscosity, 0.5 $kg \cdot m^{-3}$ for density and 0.02 K for the temperature.

3. Results

3.1. Nano-powder characterization and Ionanofluid stability

SEM images of Si_3N_4 and CB nano-powders (Figure 2) indicate that both types of nano-particles present a nearly spherical shape. The creation of the observed aggregates can be attributed to the drying process. The perceived particle sizes are in agreement with the information provided by the manufacturer (Table 1), with Si_3N_4 nano-particles being about twice as large as CB nano-particles.

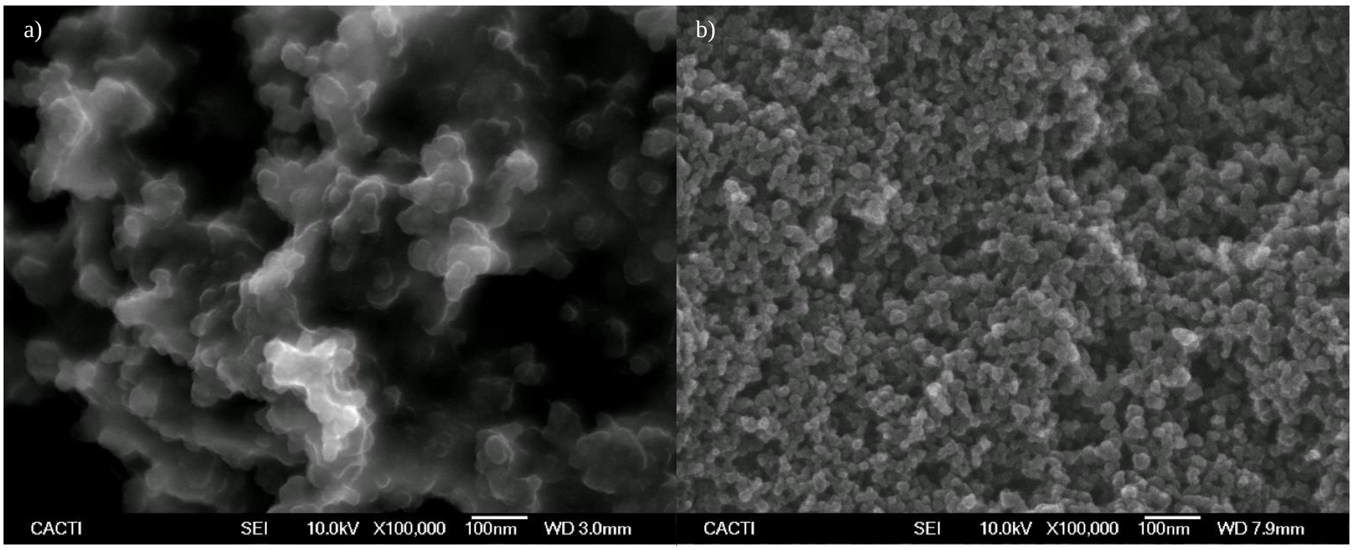

Figure 2. SEM images of Si_3N_4 (a) and CB (b) nano-particles at ×100000 magnification

With regard to the stability characterization, it is worth mentioning that the size value by DLS measurements is assumed as the diameter of a perfect sphere that presents a translational diffusion coefficient equal to that of the dispersed particle. Thus, these values are commonly referred to as hydrodynamic diameter or apparent size. On the other hand, the average Z-size is the intensity-weighted mean size calculated from a cumulants fit of the intensity autocorrelation function resulting from the DLS measurement. Therefore, it should be taken into account that the stability analysis is focused on the temporal evolution of the DLS measurements rather than the values of the sizes themselves. Figure 2 shows the average Z-size dependence on time after preparation for “static” and “shaken” 0.25 wt% Ionanofluids.

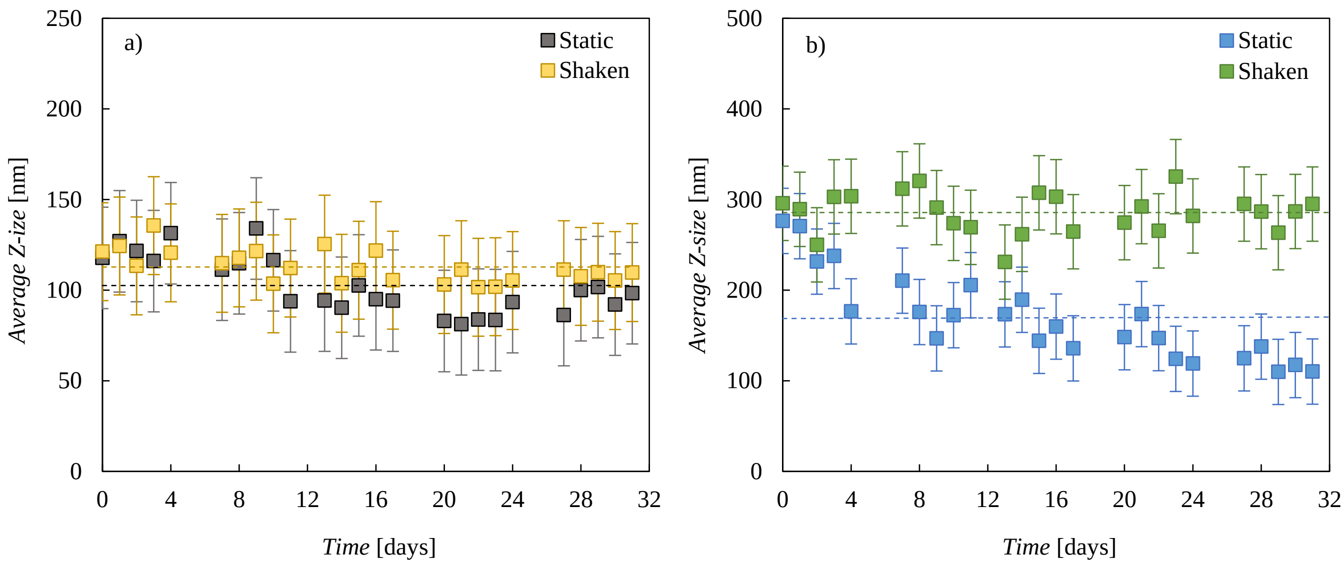

Figure 3. Average Z-size dependence on time after preparation at 298.15 K for the 0.25 wt% dispersions: Si_3N_4 Ionanofluids (a) and CB Ionanofluids (b). Error bars mean standard deviation (k=2) of the experimental measurements and reference lines (- - -) indicate the calculated average value for each sample.

Figure 3 a) indicates a quasi-constant average Z-size value during one month for "static" (~ 103 nm) and "shaken" (~ 113 nm) Si_3N_4 Ionanofluids, which is a sign of the excellent long-term stability of the dispersions. Furthermore, it should be noted that the differences between the obtained values are covered by the experimental expanded uncertainty. On the other hand, Figure 3 b) shows a marked decrease of the average Z-size with time for the "static" CB Ionanofluid while a practically constant value for the "shaken" CB Ionanofluid (~ 286 nm) during the one-month period is obtained. From these results we conclude that the largest dispersed CB nano-particles or particle agglomeration tend to precipitate in static conditions, but the initial dispersion state is easily recoverable by means of a brief mechanical agitation.

3.2. Tribological characterization

A first tribological test was performed for the six designed dispersions and the IL, in order to characterize the nano-additive mass concentration dependence on the friction coefficient, μ. Figure 4 gathers the experimental friction coefficients as a function of the sliding distance for all the samples at 353.15 K, showing that both 0.25 wt% Ionanofluid lubricants reach the highest friction coefficient reduction among those analyzed. This decrease is higher for the 0.25 wt% CB dispersion (0.089 average value, 16 % decrease) than for the 0.25 wt% Si_3N_4 dispersion (0.097 average value, 8.5 % decrease), as is also shown in Table 2 and Figure 5. Both 0.10 wt% samples (Si_3N_4 and CB-based Ionanofluids) exhibit practically the same friction behavior than the IL (an average μ value of 0.106 for [EMIM][MS] while average μ values of 0.105 and 0.103 for the corresponding Si_3N_4 and CB-based Ionanofluids, respectively). The 1.0 wt% CB dispersion presents an average μ value of 0.105, very similar to that of the IL (0.106), while the 0.25 wt% Si_3N_4 dispersion shows an average μ value of 0.123, which implies a 16 % worsening with respect to the neat IL.

The existence of an optimal nano-additive concentration for which a minimum friction coefficient is achieved was previously pointed out for other nano-lubricants [20, 21, 28, 29, 33, 46, 47, 50]. For instance, Pamies et al.[33] analyzed the tribological behavior of [EMIM][DCA] and [EMIM][TFSI] Ionanofluids, using few-layers graphene as nano-additive in the 0.5 to 1.0 wt% concentration range. They reported the highest friction reductions in comparison to the ILs for the 0.5 wt% nano-additive concentration, the lowest analyzed. Çöl et al. [41] also found an optimal friction value for dispersions of silicon nitride nano-particles in an engine oil at 0.8 wt % concentration. This friction behavior could be explained because at lower concentrations, the base oil effect governs the friction performance since the quantity of nano-particles at the contact surface is not enough to prevent wear. Meanwhile, when the nano-particle concentration is too high, nano-particle deposition can create new asperities and therefore increase the friction. In order to confirm this hypothesis, the roughness (Ra) of the worn surfaces of the lubricated pins were plotted in Figure 5 together with the friction coefficients at a function of the concentration. Both properties have minima for the dispersion of 0.25 wt% nano-additive. Thus, 75 % and 61% reductions with respect to the IL are obtained in the roughness of the worn track when the pins are lubricated with 0.25 wt% CB and Si_3N_4 Ionanofluids, respectively. Average *Ra* values are also given in Table 3. The reductions of the roughness and friction coefficients for the 0.25 wt% concentration show that polishing and mending effects occur due to the presence of nano-particles. The reduction of the friction coefficient can also be due to the rolling effect owing to the cuasi-sphericity of both types of nano-particles. In the case of CB Ionanofluids, the highest roughness reduction may be due to their small nano-particle size (13 nm) compared to Si_3N_4 (25 nm). On the other hand, when the concentration increases up to 1 wt% worn surface roughness is only 20% (CB) and 9% (Si_3N_4) lower than those obtained with those corresponding to the neat IL showing that polishing and mending effects are negatively compensated by other effects. From Figure 5 it can be concluded that 0.25 wt% of Si_3N_4 and CB Ionanofluids provide the best performance between the studied dispersions. When the concentration is lower or higher than 0.25 wt%, the friction and roughness reductions are weakened. That may be ascribed to the competitive adsorption between the additive particles and the IL. When the additive concentration is low, the particles adsorbed on the contact regions are insufficient and even serve as abrasive elements to damage the mating metal surfaces [51]. When concentration increases, more nano-particles are adsorbed onto the contact surfaces, the boundary lubricating film becomes thicker and firmer to prevent the asperities of the mating surfaces from direct contact, thus the friction and roughness decrease. Nevertheless, if the concentration increases further, many particles and aggregates are delivered onto the contact areas leading to aggregation increase at the friction interfaces due to friction force, which in turn causes the friction process to be unstable (as seen in Figure 4) and local breakage of oil film, which results in higher friction and roughness. Thus, big aggregates may scratch the surface under loading and form abrasive clusters (new asperities) between the sliding surfaces, resulting in an increase of wear [52]. In the case of Si_3N_4 these last effects are stronger because these nano-particles are harder than CB nano-particles.

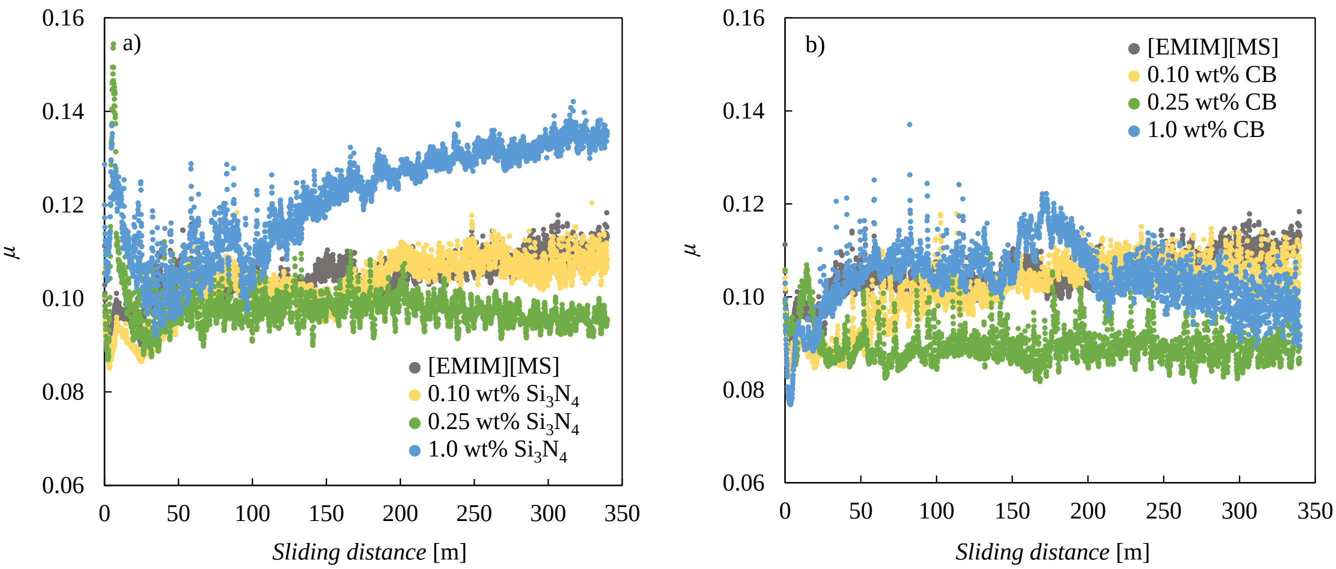

Figure 4. Friction coefficient, μ, as a function of the sliding distance at 353.15 K for [EMIM][MS] and 0.10, 0.25 and 1.0 wt% dispersions of Si_3N_4 (a) and CB (b).

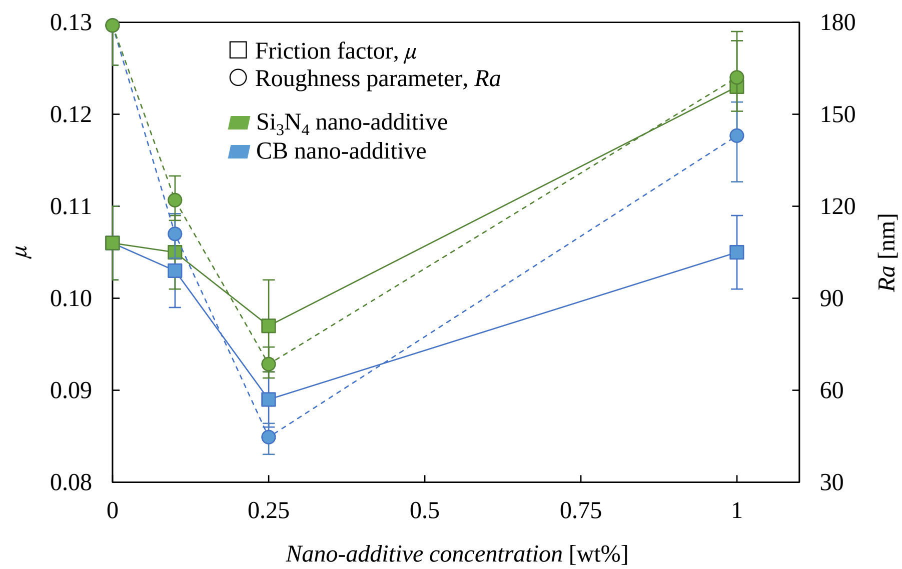

Figure 5. Average friction coefficient, μ, and Roughness parameter, *Ra*, as a function of the nano-additive concentration at 353.15 K.

Table 2. Roughness parameters, *Ra*, and the corresponding uncertainties of worn surfaces lubricated with [EMIM][MS], Si_3N_4 and CB Ionanofluids at 293.15 K (Gaussian filter of 0.08 mm) and 353.15 K (Gaussian filter of 0.25 mm).

T [K]	Lubricant	*Ra / nm*
293.15	[EMIM][MS]	25.9 (±2.4)
	0.10 wt% Si_3N_4	24.7 (±2.6)
	0.25 wt% Si_3N_4	21.4 (±2.2)
	1 wt% Si_3N_4	25.3 (±2.3)
	0.10 wt% CB	21.3 (±2.2)
	0.25 wt% CB	18.3 (±1.8)
	1 wt% CB	22.4 (±1.7)
353.15	[EMIM][MS]	179 (±13)
	0.10 wt% Si_3N_4	122 (±7.9)
	0.25 wt% Si_3N_4	68.5 (±5.6)
	1 wt% Si_3N_4	162 (±15)
	0.10 wt% CB	111 (±6.6)
	0.25 wt% CB	44.7 (±4.5)
	1 wt% CB	143 (±11)

Taking into account the previous experimental results, attention will subsequently be paid to the optimal Ionanofluids in terms of friction coefficient reduction, i.e. 0.25 wt% of Si_3N_4 and CB-based dispersions. Figure 6 and Table 3 show the friction coefficient reductions obtained by these selected dispersions at 293.15 and 353.15 K. Decreases of the friction coefficient of up to 24 % were obtained for the base fluid lowering the temperature 60 K. This behavior and the decrease in fluctuations can be explained because when the temperature decreases the viscosity increases and the lubrication film becomes wider. The following comparison between friction coefficients, μ, can be established at both temperatures: $\mu_{0.25\ wt\%\ CB} < \mu_{0.25\ wt\%\ Si3N4} < \mu_{[EMIM][MS]}$. It should be noted that the noticeable decreases in the friction coefficient found for both proposed Ionanofluids at 353.15 K are maintained at 293.15 K, but those reductions fall by half at the lower temperature.

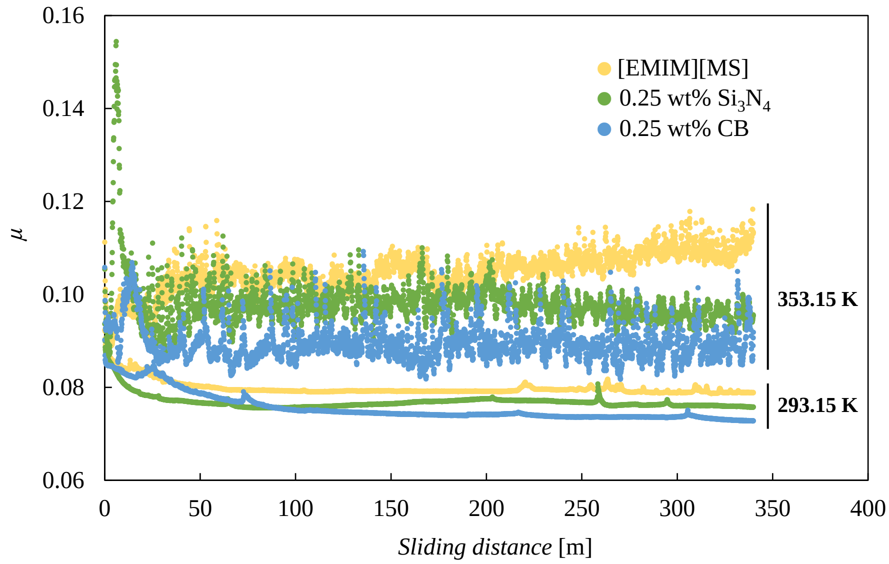

Figure 6. Friction coefficient, μ, as a function of the sliding distance for [EMIM][MS] and for 0.25 wt% Ionanofluids at 293.15 K and 353.15 K.

Table 3. Average values of friction coefficient, μ, and wear scar diameter, WSD, wear track depth, WTD, and wear hole volume, WHV, as a maximum (the respective standard deviations are shown between brackets) for [EMIM][MS], 0.25 wt% Si_3N_4 Ionanofluid and 0.25 wt% CB Ionanofluid at 293.15 and 353.15 K.

T [K]	Lubricant	μ	WSD [μm]	WTD [μm]	WHV [10^3μm^3]
	[EMIM][MS]	0.081 (±0.003)	300 (±7.5)	0.23 (±0.02)	10.3 (±0.3)
293.15	0.25 wt% Si_3N_4	0.077 (±0.003)	334 (±9.3)	0.94 (±0.06)	13.1 (±0.5)
	0.25 wt% CB	0.074 (±0.004)	247 (±5.8)	0.44 (±0.04)	10.0 (±0.3)
	[EMIM][MS]	0.106 (±0.004)	777 (±20)	10.9 (±0.47)	1951 (±64.7)
353.15	0.25 wt% Si_3N_4	0.097 (±0.005)	499 (±12)	2.98 (±0.18)	159 (±5.7)
	0.25 wt% CB	0.089 (±0.003)	421 (±14)	1.60 (±0.10)	68 (±3)

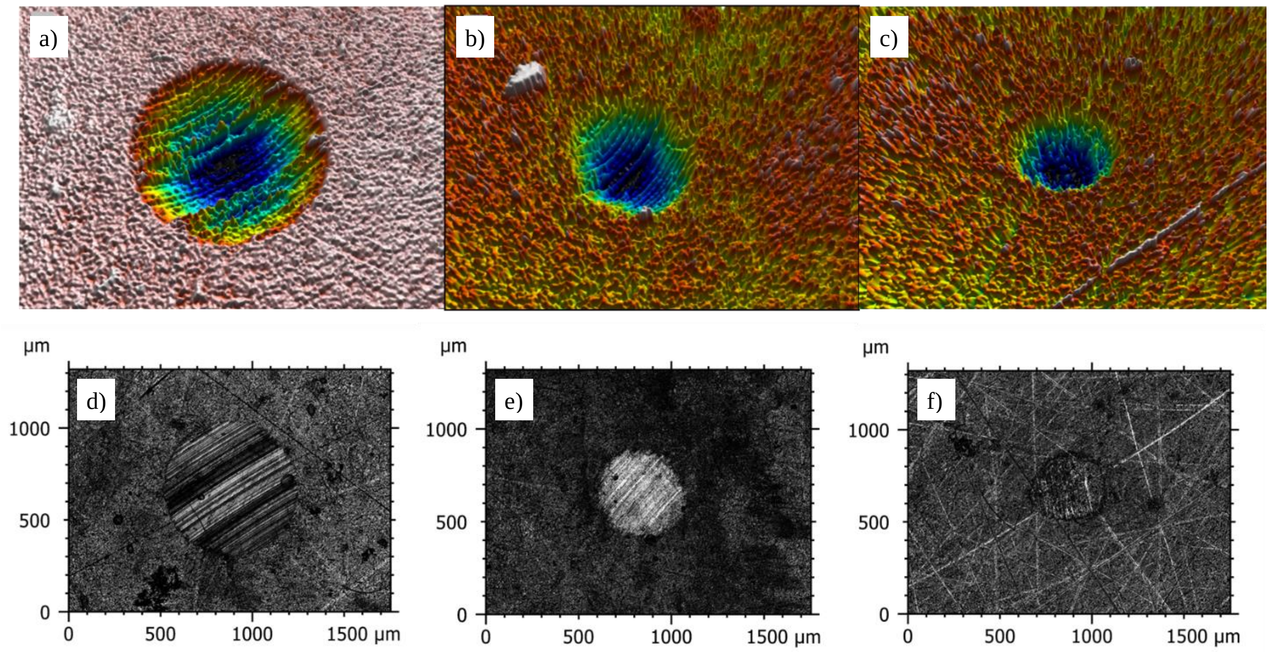

Figure 7. 3D profiles (a, b, c) and 2D images (d, e, f) of the wear tracks at 353.15 K, 10x magnification, for [EMIM][MS] (a, d), 0.25 wt% Si_3N_4 Ionanofluid (b, e) and 0.25 wt% CB Ionanofluid (c, f).

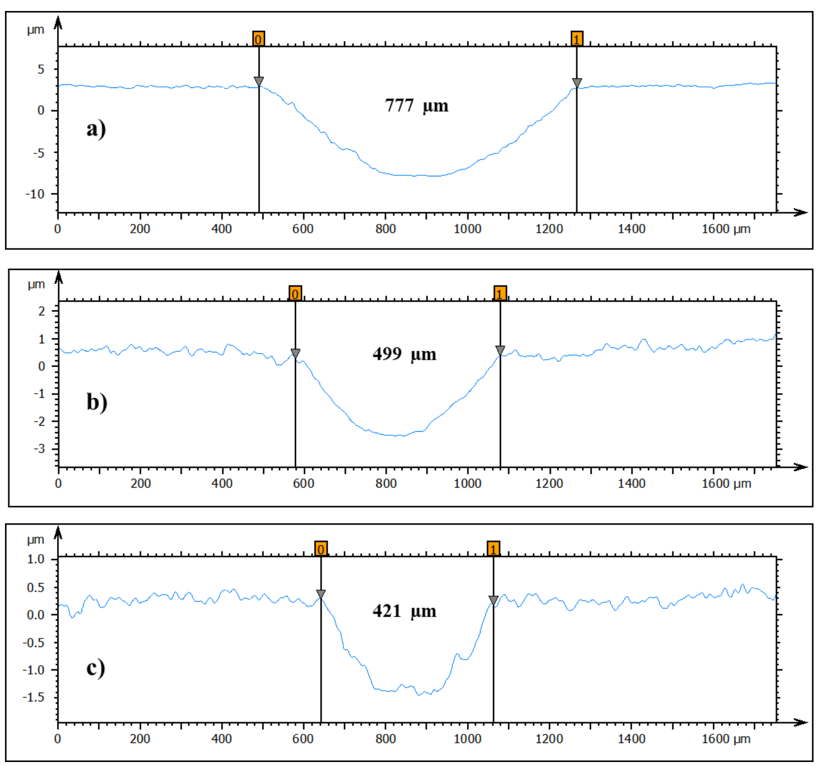

Figure 8. Cross section profiles of the wear tracks with the corresponding wear scar diameters (WSD) at 353.15 K for [EMIM][MS] (a), 0.25 wt% Si_3N_4 Ionanofluid (b) and 0.25 wt% CB Ionanofluid (c).

As presented in Table 3, the obtained wears at the lowest temperature are very similar for all lubricants in terms of wear scar diameter, WSD, wear track depth, WTD, or wear hole volume, WHV. Contrarily, these values at the highest temperature are much lower for the Ionanofluids than for the base IL, as Figures 7 and 8 specifically show. In particular, reductions of 46 and 85% were achieved for the pins lubricated with the 0.25 wt% CB Ionanofluid in WSD and WTD, respectively (being the mean WHV more than 28 times lower). As regards pins lubricated with 0.25 wt% Si_3N_4 Ionanofluid, reductions of 36 and 73% in WSD and WTD, respectively, were obtained (WHV more than 12 times lower).

The elemental mapping and Raman spectra of the worn surfaces lubricated with the 0.25 wt% CB and 0.25 wt% Si_3N_4 Ionanofluids were carried out to identify the role that the nano-particles and ionic liquid play in the reduction of the surface wear of the pins. As it is presented in Figure 9, an important tribofilm is evidenced due to a significant presence of IL (blue color) in the mapping of the worn surfaces lubricated with both nanolubricants. The IL contains “aromatic” C–H units with distinctive stretching modes associated to peaks between 3070–3200 cm^{-1} and it has characteristic bands in the region 1450–1570 cm^{-1} and at about 1150–1370 cm^{-1} [53]. As regards the methanesulfonate anion the characteristic Raman frequencies are assigned to symmetric and asymmetric stretching vibrations, $\nu_s(SO_3)$ and $\nu_{as}(SO_3)$, between 1050 and 1200cm^{-1} [53].

Moreover, a clear presence of CB nano-particles appears on the worn surface lubricated with 0.25 wt% CB Ionanofluid (Figure 9b), these nano-additives are placed along several furrows on the worn surface. Characteristic peaks of CB nano-particles are identified in the Raman spectrum of worn surface: carbon black generally exhibits two broad and strongly overlapping peaks with intensity maxima at around 1350 cm^{-1} and around 1585 cm^{-1}, which are associated to the defect band (D band) and the graphite band (G band) [54, 55]. The presence of CB nano-particles as well as the reduction in roughness could indicate the occurrence of mending effect due to the CB nano-particles. Regarding the worn surface lubricated with 0.25 wt% Si_3N_4 Ionanofluid, no physical adsorption of the nano-particles is observed (Figure 9a). Therefore, the wear reduction may be mainly due to rolling and the polishing effects because of the nearly spherical shape and high hardness of Si_3N_4 nano-particles, respectively.

a)

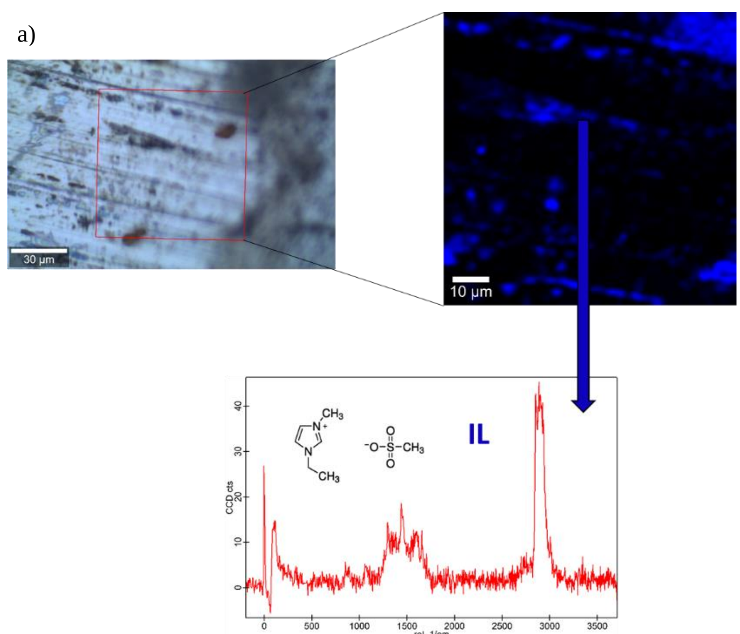

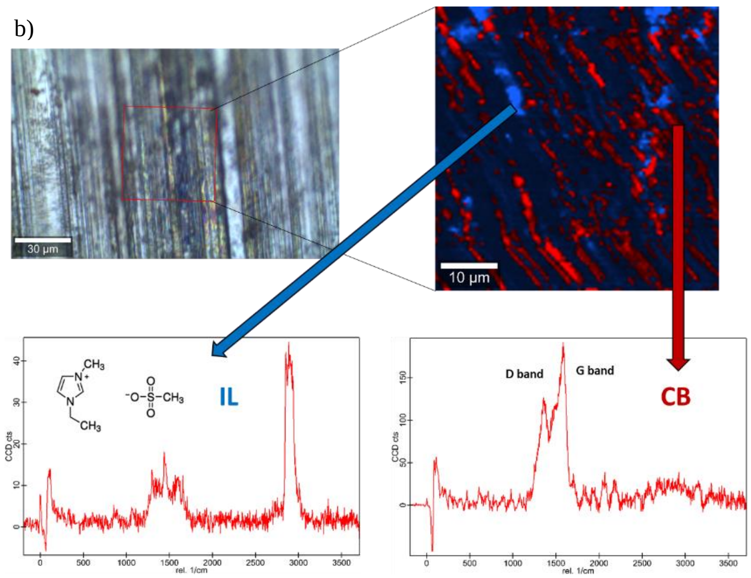

Figure 9. Raman spectra and elemental map of the worn surface obtained with the 0.25 wt% Si_3N_4 Ionanofluid (a) and the 0.25 wt% CB Ionanofluid (b).

3.3. Density and dynamic viscosity

Figure 10a shows that experimental density values for [EMIM][MS] (reported in Table 4) are in agreement with the corresponding literature data [37, 40, 56-68], with absolute average deviations within 0.4%. It should be noted that the content of water is slightly different among the reported literature, but always less than 1% [37, 40, 56-68]. The best agreements were found with the data from Domanska et al. [60], Rabari et al. [64], Krannich et al. [40], Marium et al. [66], and Chereches et al. [68], with absolute average deviations of 0.03%, 0.10%, 0.09%, 0.02% and 0.05%, respectively.

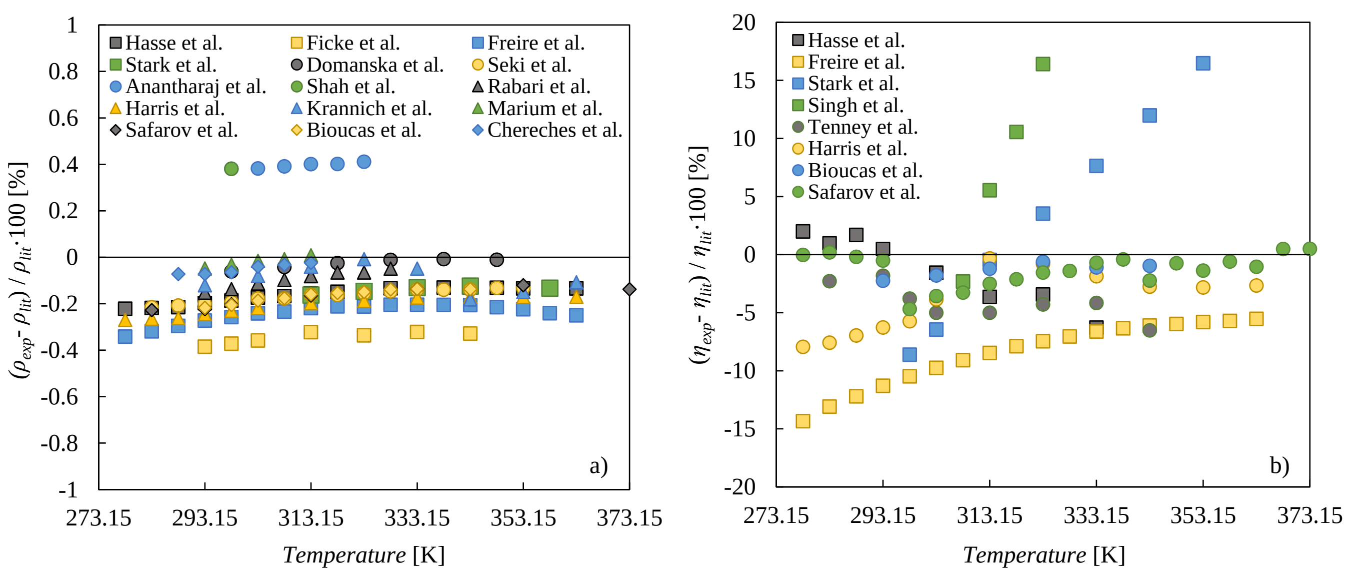

Figure 10. Relative deviations between experimental, *exp*, and literature, *lit*, data as a function of temperature for [EMIM][MS] for density, ρ, [37, 40, 56-68] (a), and dynamic viscosity, η, [37, 56, 58, 59, 65, 69-71] (b).

Table 4 shows the experimental density values of the optimal nano-additive loading dispersions for the friction reduction, the 0.25 wt% Ionanofluids. The base fluid and both Ionanofluids show a density decrease of 5.0% with the temperature rising from 278.15 to 373.15 K. On the other hand, the dispersion of Si_3N_4 and CB caused almost temperature independent increases in the densities around 0.14% and 0.10%, respectively. Increases in mass per unit volume can lead to additional difficulties in fluid flow. The reported density increases for the selected improved dispersions are less than 0.15% in both cases, a slight variation that does not involve a noticeable change in relation to the base fluid.

Table 4. Experimental densities, *ρ*, for [EMIM][MS], 0.25 wt% Si_3N_4 Ionanofluid and 0.25 wt% CB Ionanofluid at temperatures, *T*, from 278.15 to 373.15 K and fitting parameters, A_0, A_1, A_2, standard deviations, s, and absolute average deviations, AAD, from Eq. (1).

T [K]	*ρ* [kg·m^{-3}]		
	[EMIM][MS]	0.25 wt% Si_3N_4	0.25 wt% CB
278.15	1252.8	1254.9	1254.3
283.15	1249.3	1251.3	1250.7
288.15	1245.8	1247.9	1247.2
293.15	1242.5	1244.5	1243.8
298.15	1239.2	1241.1	1240.5
303.15	1236.0	1237.8	1237.2
308.15	1232.7	1234.5	1234.0
313.15	1229.5	1231.2	1230.7
318.15	1226.2	1227.9	1227.4
323.15	1222.9	1224.6	1224.1
328.15	1219.7	1221.2	1220.8
333.15	1216.4	1217.9	1217.5
338.15	1213.1	1214.6	1214.2
343.15	1209.8	1211.3	1210.9
348.15	1206.5	1208.0	1207.6
353.15	1203.2	1204.7	1204.3
358.15	1199.9	1201.4	1201.1
363.15	1196.7	1198.2	1197.8
368.15	1193.4	1194.9	1194.5
373.15	1190.2	1191.7	1191.3
A_0 [kg·m^{-3}]	1435.1	1439.1	1437.5
-A_1 [kg·m^{-3}·K^{-1}]	0.6566	0.6636	0.6602
10^9·A_2 [kg·m^{-3}·K^{-2}]	2.824	5.891	7.324
s [kg·m^{-3}]	0.11	0.14	0.14
AAD	0.006%	0.008%	0.008%

The temperature dependence on density was correlated by the following quadratic equation:

$$\rho(T) = A_2 \cdot T^2 + A_1 \cdot T + A_0 \qquad (1)$$

where ρ and T means density and temperature, respectively, and A_2, A_1 and A_0 are the fitting parameters. The values of the fitting parameters reported in Table 4 allow for a correlation of the experimental density data with standard deviations lower than 0.15 $kg \cdot m^{-3}$ for all samples. Isobaric thermal expansivity at atmospheric pressure was obtained by the following equation [72, 73]:

$$\alpha_p = -\frac{1}{\rho} \cdot \left(\frac{d\rho}{dT} \right)_p \tag{2}$$

Figure 11 gathers the obtained isobaric thermal expansivities in the temperature range from 283.15 to 368.15 K. Rises with the temperature increase of 4.7% were detected for base fluid and Ionanofluids. The nano-additive dispersion leads to higher thermal expansivity values. Increases for the 0.25 wt% Si_3N_4 and CB loadings of around 0.92 % and 0.45% were obtained, respectively. Isobaric thermal expansivity values are useful to determine the size of the container when the fluid is heated. As observed, the differences between Ionanofluids and base IL are lower than 1% in both cases.

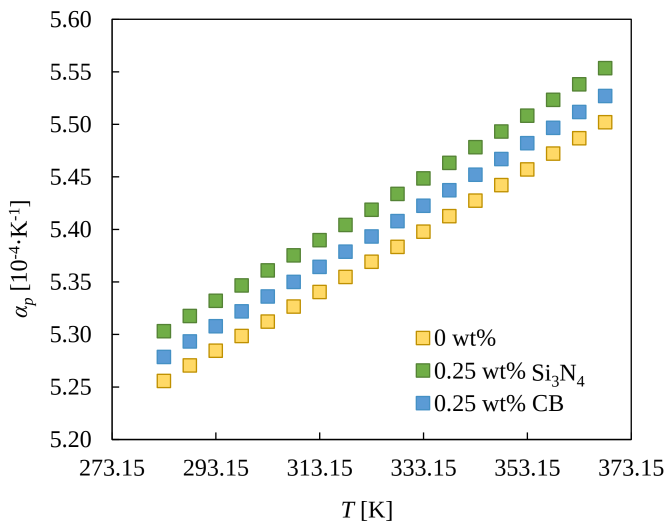

Figure 11. Isobaric thermal expansivity, αp, as a function of temperature, T, for [EMIM][MS], 0.25 wt% Si3N4 Ionanofluid and 0.25 wt% CB Ionanofluid**.**

Figure 10b shows the relative deviations between the experimental dynamic viscosities for [EMIM][MS] (Table 5) and the corresponding literature data [37, 56, 58, 59, 65, 69-71]. It should be noted that some data sets present large deviations from the rest of the literature data, with significant dependence on temperature. The absolute average deviations between the experimental dynamic viscosity data reported in this work and those from Tenney et al. [70] and Harris et al. [65] are within 4.2%. The best agreements were found with Hasse et al. [56], Bioucas et al. [37] and Safarov et al [71], with absolute average deviations of 2.5%, 1.5% and 1.4%, respectively.

Table 5 also reports the experimental dynamic values of the optimal nano-additive loading dispersions for the friction reduction. The increasing temperature from 278.15 to 373.15 K leads to a dynamic viscosity reduction of 99% for [EMIM][MS] and both Ionanofluids. Contrastingly, increases in the ranges 3.5-6.3% and 5.2-12% at constant temperature were observed because of the dispersion of Si_3N_4 and CB in the base fluid, respectively. These increases tend to be lower as the temperature rises. Viscosity is directly related to the energy required to make a fluid flow. Small increases in dynamic viscosity were obtained for both selected Ionanofluids, where the increment for Si_3N_4 Ionanofluid is half of that for CB Ionanofluid. The CB dispersion, which allows for a greater improvement in the friction coefficient and scar wear, implies a higher increase in viscosity and, therefore, a slightly higher pumping power.

Table 5. Experimental dynamic viscosities, η, for [EMIM][MS], 0.25 wt% Si_3N_4 Ionanofluid and 0.25 wt% CB Ionanofluid at temperatures, T, from 278.15 to 373.15 K and fitting parameters, η_0, A and T_0, standard deviations, s, and absolute average deviations, AAD, from Eq. (3).

T [K]	η [mPa·s]		
	[EMIM][MS]	0.25 wt% Si_3N_4	0.25 wt% CB
278.15	689.8	732.9	772.3
283.15	439.7	465.6	492.0
288.15	295.0	311.0	329.6
293.15	206.2	216.7	230.1
298.15	149.1	156.2	166.2
303.15	111.1	116.1	123.5
308.15	84.98	88.59	94.26
313.15	66.49	69.15	73.52
318.15	53.07	55.09	58.43
323.15	43.07	44.67	47.26
328.15	35.51	36.78	38.82
333.15	29.70	30.73	32.29
338.15	25.13	26.01	27.19
343.15	21.50	22.26	23.14
348.15	18.57	19.23	19.91
353.15	16.19	16.77	17.28
358.15	14.22	14.73	15.11
363.15	12.59	13.05	13.32
368.15	11.22	11.64	11.82
373.15	10.06	10.44	10.58
η_0	0.2392	0.2339	0.2301
A [K]	3.447	3.492	3.608
T_0 [K]	194.1	194.0	192.6
s [mPa·s]	0.33	0.36	0.42
AAD	0.4%	0.9%	0.6%

The temperature dependence on the dynamic viscosity was correlated by the Vogel–Fulcher–Tammann (VFT) equation [74-76], or Vogel–Fulcher–Tammann–Hesse equation:

$$\eta = \eta_0 \cdot e^{\frac{A \cdot T_0}{T - T_0}} \tag{3}$$

where η and T means dynamic viscosity and temperature, respectively, and η_0, A and T_0 are the fitting parameters. The values of the fitting parameters gathered in Table 5 allow for the correlation of the experimental dynamic viscosity data with absolute average deviations of less than 1%.

4. Conclusions

In this work the following features were achieved:

1. New Si_3N_4 and CB dispersions in [EMIM][MS] at nano-particle mass concentration between 0.1 to 1 % were conveniently designed for lubrication purposes.
2. DLS measurements indicated the excellent long-term stability of the Si_3N_4 Ionanofluids and the easily recoverable initial dispersion conditions of the CB Ionanofluids.
3. Ionanofluids at 0.25 wt% mass concentration achieved the highest friction coefficient reductions at both analyzed temperatures, 293.15 and 353.15 K. At the highest temperature, these decreases reached 16% and 8.5% for the CB and Si_3N_4 dispersions, respectively.
4. The maximum wear reductions were produced at 353.15K: the 0.25 wt% CB Ionanofluid achieved 46% and 85% in the diameter and depth of the wear, respectively, whereas 36% and 73% reductions were respectively obtained for the 0.25 wt% Si_3N_4 Ionanofluid. The maximum volume reduction was achieved for the 0.25 wt% CB Ionanofluid with 28 times lower wear volume than that for the base IL.
5. The roughness of the worn surfaces achieves 75% and 61% reductions by using the 0.25 wt% CB and Si_3N_4 new lubricants, respectively.
6. Raman mapping indicates that mending effect occurs using the optimal CB Ionanofluid, but does not show this effect for the optimal Si_3N_4 dispersion.
7. Dynamic viscosity rises lower or equal to 6.3% and 12% for the 0.25 wt% Si_3N_4 and CB Ionanofluids were reached, whereas density increases up to around 0.14% and 0.10%, respectively, with almost no dependence on temperature.

CRediT authorship contribution statement

Javier P. Vallejo: Conceptualization, Investigation, Methodology, Writing - original draft, Writing - review & editing. **José M. Liñeira del Río**: Investigation, Methodology, Writing - original draft. **Josefa Fernández**: Conceptualization, Supervision, Validation, Writing - review & editing. **Luis Lugo**: Conceptualization, Supervision, Validation, Writing - review & editing.

Declaration of competing interest

There is no conflict of interest.

Acknowledgements

This work was supported by the "Ministerio de Economía y Competitividad" (Spain) and the ERDF program through ENE2017-86425-C2-1/2-R projects, and by the "Xunta de Galicia" (ED431E2018/08, ED431D 2017/06 and GRC ED431C 2016/001). J.P.V. acknowledges the FPI Program of the "Ministerio de Economía y Competitividad".

References

[1] J.P. Vallejo, E. Álvarez-Regueiro, D. Cabaleiro, J. Fernández-Seara, J. Fernández, L. Lugo, Functionalized graphene nanoplatelet nanofluids based on a commercial industrial antifreeze for the thermal performance enhancement of wind turbines, Appl.Therm. Eng. 152 (2019) 113.

[2] J.P. Vallejo, G. Żyła, J. Fernández-Seara, L. Lugo, Influence of six carbon-based nanomaterials on the rheological properties of nanofluids, Nanomaterials 9 (2019) 146.

[3] W. Dai, B. Kheireddin, H. Gao, H. Liang, Roles of nanoparticles in oil lubrication, Tribol. Int. 102 (2016) 88.

[4] A. Kotia, P. Rajkhowa, G.S. Rao, S.K. Ghosh, Thermophysical and tribological properties of nanolubricants: A review, Heat Mass Transfer 54 (2018) 3493.
[5] G. Paul, H. Hirani, T. Kuila, N.C. Murmu, Nanolubricants dispersed with graphene and its derivatives: an assessment and review of the tribological performance, Nanoscale 11 (2019) 3458.
[6] A. Singh, P. Chauhan, T.G. Mamatha, A review on tribological performance of lubricants with nanoparticles additives, Mater. Today Proc. 25 (2020) 586.
[7] Z. Tang, S. Li, A review of recent developments of friction modifiers for liquid lubricants (2007–present), Curr. Opin. Solid St. M. 18 (2014) 119.
[8] P. Oulego, J. Faes, R. González, J.L. Viesca, D. Blanco, A.H. Battez, Relationships between the physical properties and biodegradability and bacteria toxicity of fatty acid-based ionic liquids, J. Mol. Liq. 292 (2019) 111451.
[9] T. Regueira, L. Lugo, J. Fernández, Ionic liquids as hydraulic fluids: comparison of several properties with those of conventional oils, Lubr. Sci. 26 (2014) 488.
[10] H. Xiao, Ionic liquid lubricants: basics and applications, Tribol. Trans. 60 (2017) 20.
[11] I. Otero, E.R. López, M. Reichelt, M. Villanueva, J. Salgado, J. Fernández, Ionic liquids based on phosphonium cations as neat lubricants or lubricant additives for a steel/steel contact, ACS Appl. Mater. Interfaces 6 (2014) 13115.
[12] Y. Zhou, J. Qu, Ionic Liquids as Lubricant Additives: A Review, ACS Appl. Mater. Interfaces 9 (2017) 3209.
[13] S. Kawada, Y. Ichise, S. Watanabe, C. Tadokoro, S. Sasaki, in: G. Biresaw, K.L. Mittal (Eds.), Surfactants in Tribology, CRC Press, Boca Raton, FL, USA, 2017.
[14] P. Oulego, D. Blanco, D. Ramos, J.L. Viesca, M. Díaz, A. Hernández Battez, Environmental properties of phosphonium, imidazolium and ammonium cation-based ionic liquids as potential lubricant additives, J. Mol. Liq. 272 (2018) 937.
[15] A. Ribeiro, M. Lourenço, C.N. de Castro, 17th symposium on thermophysical properties, Boulder, USA, 2009.
[16] B. Jóźwiak, S. Boncel, Rheology of ionanofluids–A review, J. Mol. Liq. 302 (2020) 112568.
[17] C. Hermida-Merino, A. Pereiro, J. Araújo, C. Gracia-Fernández, J.P. Vallejo, L. Lugo, M. Piñeiro, Graphene IoNanofluids, Thermal and Structural Characterization, Nanomaterials 9 (2019) 1549.
[18] B. Bakthavatchalam, K. Habib, R. Saidur, B.B. Saha, K. Irshad, Comprehensive study on nanofluid and ionanofluid for heat transfer enhancement: A review on current and future perspective, J. Mol. Liq. 305 (2020) 112787.
[19] A. Hosseinghorbani, M. Mozaffarian, G. Pazuki, Application of graphene oxide IoNanofluid as a superior heat transfer fluid in concentrated solar power plants, Int. Commun. Heat Mass 111 (2020) 104450.
[20] B. Wang, X. Wang, W. Lou, J. Hao, Gold-ionic liquid nanofluids with preferably tribological properties and thermal conductivity, Nanoscale Res. Lett. 6 (2011) 1.
[21] X. Liu, J. Pu, L. Wang, Q. Xue, Novel DLC/ionic liquid/graphene nanocomposite coatings towards high-vacuum related space applications, J. Mater. Chem. A 1 (2013) 3797.
[22] L. Zhang, J. Pu, L. Wang, Q. Xue, Synergistic effect of hybrid carbon nanotube–graphene oxide as nanoadditive enhancing the frictional properties of ionic liquids in high vacuum, ACS Appl. Mater. Interfaces 7 (2015) 8592.
[23] N. Saurín, J. Sanes, M.D. Bermúdez, New graphene/ionic liquid nanolubricants, Mater. Today Proc. 3 (2016) 227.
[24] I. Minami, M. Kita, T. Kubo, H. Nanao, S. Mori, The tribological properties of ionic liquids composed of trifluorotris (pentafluoroethyl) phosphate as a hydrophobic anion, Tribol. Lett. 30 (2008) 215.
[25] M.G. Freire, C.M. Neves, I.M. Marrucho, J.A. Coutinho, A.M. Fernandes, Hydrolysis of tetrafluoroborate and hexafluorophosphate counter ions in imidazolium-based ionic liquids, J. Phys. Chem. A 114 (2010) 3744.
[26] I. Otero, E.R. López, M. Reichelt, J. Fernández, Tribo-chemical reactions of anion in pyrrolidinium salts for steel–steel contact, Tribol. Int. 77 (2014) 160.
[27] V. Khare, M.Q. Pham, N. Kumari, H.S. Yoon, C.S. Kim, J.I. Park, S.H. Ahn, Graphene–ionic liquid based hybrid nanomaterials as novel lubricant for low friction and wear, ACS Appl. Mater. Interfaces 5 (2013) 4063.
[28] B.A. Kheireddin, W. Lu, I.C. Chen, M. Akbulut, Inorganic nanoparticle-based ionic liquid lubricants, Wear 303 (2013) 185.
[29] C. Yegin, W. Lu, B. Kheireddin, M. Zhang, P. Li, Y. Min, H.J. Sue, M. Murat Sari, M. Akbulut, The effect of nanoparticle functionalization on lubrication performance of nanofluids dispersing silica nanoparticles in an ionic liquid, J. Tribol. 139 (2017).
[30] F.J. Carrión, J. Sanes, M.D. Bermúdez, A. Arribas, New single-walled carbon nanotubes–ionic liquid lubricant. Application to polycarbonate–stainless steel sliding contact, Tribol. Lett. 41 (2011) 199.
[31] C. Espejo, F.J. Carrión, D. Martínez, M.D. Bermúdez, Multi-walled carbon nanotube-imidazolium tosylate ionic liquid lubricant, Tribol. Lett. 50 (2013) 127.
[32] N. Saurín, M. Avilés, T. Espinosa, J. Sanes, F. Carrión, M. Bermúdez, P. Iglesias, Carbon nanophases in ordered nanofluid lubricants, Wear 376 (2017) 747.
[33] R. Pamies, M. Avilés, J. Arias Pardilla, T. Espinosa, F. Carrión, J. Sanes, M. Bermúdez, Antiwear performance of ionic liquid+ graphene dispersions with anomalous viscosity-temperature behavior, Tribol. Int. 122 (2018) 200.

[34] M.D. Avilés, N. Saurín, J. Sanes, F.J. Carrión, M.D. Bermúdez, Ionanocarbon lubricants. The combination of ionic liquids and carbon nanophases in tribology, Lubricants 5 (2017) 14.
[35] J. Zhao, Y. He, Y. Wang, W. Wang, L. Yan, J. Luo, An investigation on the tribological properties of multilayer graphene and MoS2 nanosheets as additives used in hydraulic applications, Tribol. Int. 97 (2016) 14.
[36] T. Predel, E. Schluecker, Ionic liquids in oxygen compression, Chem. Eng. Technol. 32 (2009) 1183.
[37] F. Bioucas, S. Vieira, M. Lourenço, F. Santos, C. Nieto de Castro, K. Massonne, [C_2mim][CH_3SO_3] – A suitable new heat transfer fluid? Part 1. Thermophysical and toxicological properties, Ind. Eng. Chem. Res. 57 (2018) 8541.
[38] G. Stachowiak, A.W. Batchelor, Engineering tribology. 4th edn. Butterworth-Heinemann, Massachusetts, USA, 2013.
[39] M. Musiał, M. Zorębski, M. Dzida, J. Safarov, E. Zorębski, E. Hassel, High pressure speed of sound and related properties of 1-ethyl-3-methylimidazolium methanesulfonate, J. Mol. Liq. 276 (2019) 885.
[40] M. Krannich, F. Heym, A. Jess, Characterization of six hygroscopic ionic liquids with regard to their suitability for gas dehydration: density, viscosity, thermal and oxidative stability, vapor pressure, diffusion coefficient, and activity coefficient of water, J. Chem. Eng. Data 61 (2016) 1162.
[41] M. Çöl, O. Çelik, A. Sert, Tribological behaviors of lubricating oils with CNT and Si_3N_4 nanoparticle additives, Arch. Mater. Sci. Eng. 67 (2014) 53.
[42] J.P. Vallejo, L. Mercatelli, M.R. Martina, D. Di Rosa, A. Dell'Oro, L. Lugo, E. Sani, Comparative study of different functionalized graphene-nanoplatelet aqueous nanofluids for solar energy applications, Renew. Energy 141 (2019) 791.
[43] J.P. Vallejo, E. Sani, G. Żyła, L. Lugo, Tailored silver/graphene nanoplatelet hybrid nanofluids for solar applications, J. Mol. Liq. 296 (2019) 112007.
[44] K.I. Nasser, J.M.L. del Río, E.R. López, J. Fernández, Synergistic effects of hexagonal boron nitride nanoparticles and phosphonium ionic liquids as hybrid lubricant additives, J. Mol. Liq. 311 (2020) 113343.
[45] J.M. Liñeira del Río, E.R. López, M. González Gómez, S. Yáñez Vilar, Y. Piñeiro, J. Rivas, D.E. Gonçalves, J.H. Seabra, J. Fernández, Tribological behavior of nanolubricants based on coated magnetic nanoparticles and trimethylolpropane trioleate base oil, Nanomaterials 10 (2020) 683.
[46] J.M. Liñeira del Río, E.R. López, J. Fernández, F. García, Tribological properties of dispersions based on reduced graphene oxide sheets and trimethylolpropane trioleate or PAO 40 oils, J. Mol. Liq. 274 (2019) 568.
[47] J.M. Liñeira del Río, M.J. Guimarey, M.J. Comuñas, E.R. López, A. Amigo, J. Fernández, Thermophysical and tribological properties of dispersions based on graphene and a trimethylolpropane trioleate oil, J. Mol. Liq. 268 (2018) 854.
[48] X. Paredes, O. Fandiño, M.J. Comuñas, A.S. Pensado, J. Fernández, Study of the effects of pressure on the viscosity and density of diisodecyl phthalate, J. Chem.Thermodyn. 41 (2009) 1007.
[49] F.M. Gaciño, T. Regueira, L. Lugo, M.J. Comuñas, J. Fernández, Influence of molecular structure on densities and viscosities of several ionic liquids, J. Chem. Eng. Data 56 (2011) 4984.
[50] J.M. Liñeira del Río, M.J. Guimarey, M.J. Comuñas, E.R. López, J.I. Prado, L. Lugo, J. Fernández, Tribological and Thermophysical Properties of Environmentally-Friendly Lubricants Based on Trimethylolpropane Trioleate with Hexagonal Boron Nitride Nanoparticles as an Additive, Coatings 9 (2019) 509.
[51] B. Zhang, Y. Xu, F. Gao, P. Shi, B. Xu, Y. Wu, Sliding friction and wear behaviors of surface-coated natural serpentine mineral powders as lubricant additive, Appl. Surf. Sci. 257 (2011) 2540.
[52] C. Zhao, Y. Chen, G. Ren, A study of tribological properties of water-based ceria nanofluids, Tribol. Trans. 56 (2013) 275.
[53] M. Gjikaj, W. Brockner, J. Namyslo, A. Adam, Crown-ether enclosure generated by ionic liquid components—synthesis, crystal structure and Raman spectra of compounds of imidazolium based salts and 18-crown-6, Cryst Eng Comm 10 (2008) 103.
[54] S. Hu, F. Tian, P. Bai, S. Cao, J. Sun, J. Yang, Synthesis and luminescence of nanodiamonds from carbon black, Mater. Sci. Eng. B 157 (2009) 11.
[55] L. Bokobza, J.-L. Bruneel, M. Couzi, Raman spectra of carbon-based materials (from graphite to carbon black) and of some silicone composites, C J. Carbon Res. 1 (2015) 77.
[56] B. Hasse, J. Lehmann, D. Assenbaum, P. Wasserscheid, A. Leipertz, A.P. Fröba, Viscosity, interfacial tension, density, and refractive index of ionic liquids [EMIM][$MeSO_3$], [EMIM][$MeOHPO_2$], [EMIM][$OcSO_4$], and [BBIM][NTf_2] in dependence on temperature at atmospheric pressure, J. Chem. Eng. Data 54 (2009) 2576.
[57] L.E. Ficke, R.R. Novak, J.F. Brennecke, Thermodynamic and thermophysical properties of ionic liquid+ water systems, J. Chem. Eng. Data 55 (2010) 4946.
[58] M.G. Freire, A.R.R. Teles, M.A. Rocha, B. Schröder, C.M. Neves, P.J. Carvalho, D.V. Evtuguin, L.M. Santos, J.A. Coutinho, Thermophysical characterization of ionic liquids able to dissolve biomass, J. Chem. Eng. Data 56 (2011) 4813.
[59] A. Stark, A.W. Zidell, M.M. Hoffmann, Is the ionic liquid 1-ethyl-3-methylimidazolium methanesulfonate [emim][$MeSO_3$] capable of rigidly binding water?, J. Mol. Liq. 160 (2011) 166.
[60] U. Domańska, M. Królikowski, Measurements of activity coefficients at infinite dilution for organic solutes and water in the ionic liquid 1-ethyl-3-methylimidazolium methanesulfonate, J. Chem. Thermodyn. 54 (2012) 20.

[61] S. Seki, S. Tsuzuki, K. Hayamizu, Y. Umebayashi, N. Serizawa, K. Takei, H. Miyashiro, Comprehensive refractive index property for room-temperature ionic liquids, J. Chem. Eng. Data 57 (2012) 2211.

[62] R. Anantharaj, T. Banerjee, Thermodynamic properties of 1-ethyl-3-methylimidazolium methanesulphonate with aromatic sulphur, nitrogen compounds at T= 298.15–323.15 K and P= 1 bar, Can. J. Chem. Eng. 91 (2013) 245.

[63] M.R. Shah, R. Anantharaj, T. Banerjee, G.D. Yadav, Quaternary (liquid+ liquid) equilibria for systems of imidazolium based ionic liquid+ thiophene+ pyridine+ cyclohexane at 298.15 K: Experiments and quantum chemical predictions, J. Chem. Thermodyn. 62 (2013) 142.

[64] D. Rabari, N. Patel, M. Joshipura, T. Banerjee, Densities of six commercial ionic liquids: experiments and prediction using a cohesion based cubic equation of state, J. Chem. Eng. Data 59 (2014) 571.

[65] K.R. Harris, M. Kanakubo, Self-diffusion coefficients and related transport properties for a number of fragile ionic liquids, J. Chem. Eng. Data 61 (2016) 2399.

[66] M. Marium, A. Auni, M.M. Rahman, M.Y.A. Mollah, M.A.B.H. Susan, Molecular level interactions between 1-ethyl-3-methylimidazolium methanesulphonate and water: Study of physicochemical properties with variation of temperature, J. Mol. Liq. 225 (2017) 621.

[67] J. Safarov, G. Huseynova, M. Bashirov, E. Hassel, I. Abdulagatov, High temperatures and high pressures density measurements of 1-ethyl-3-methylimidazolium methanesulfonate and Tait-type equation of state, J. Mol. Liq. 238 (2017) 347.

[68] E.I. Cherecheş, J.I. Prado, M. Cherecheş, A.A. Minea, L. Lugo, Experimental study on thermophysical properties of alumina nanoparticle enhanced ionic liquids, J. Mol. Liq. 291 (2019) 111332.

[69] M.P. Singh, S.K. Mandal, Y.L. Verma, A.K. Gupta, R.K. Singh, S. Chandra, Viscoelastic, surface, and volumetric properties of ionic liquids [BMIM][$OcSO_4$], [BMIM][PF_6], and [EMIM][$MeSO_3$], J. Chem. Eng. Data 59 (2014) 2349.

[70] C.M. Tenney, M. Massel, J.M. Mayes, M. Sen, J.F. Brennecke, E.J. Maginn, A computational and experimental study of the heat transfer properties of nine different ionic liquids, J. Chem. Eng. Data 59 (2014) 391.

[71] J. Safarov, G. Huseynova, M. Bashirov, E. Hassel, I. Abdulagatov, Viscosity of 1-ethyl-3-methylimidazolium methanesulfonate over a wide range of temperature and Vogel–Tamman–Fulcher model, Phys. Chem. Liq. 56 (2018) 703.

[72] E. Aicart, E. Junquera, T.M. Letcher, Isobaric thermal expansivity and isothermal compressibility of several nonsaturated hydrocarbons at 298.15 K, J. Chem. Eng. Data 40 (1995) 1225.

[73] J.P. Vallejo, J. Pérez-Tavernier, D. Cabaleiro, J. Fernández-Seara, L. Lugo, Potential heat transfer enhancement of functionalized graphene nanoplatelet dispersions in a propylene glycol-water mixture. Thermophysical profile, J. Chem. Thermodyn. 123 (2018) 174.

[74] H. Vogel, The law of the relation between the viscosity of liquids and the temperature, Phys. Z 22 (1921) 645.

[75] G.S. Fulcher, Analysis of recent measurements of the viscosity of glasses, J. Am. Ceram. Soc. 8 (1925) 339.

[76] G. Tammann, W. Hesse, The dependence of viscosity upon the temperature of supercooled liquids, Z. Anorg. Allg. Chem. 156 (1926) 245.